Two-photon vibrational spectroscopy for biosciences based on surface-enhanced hyper-Raman scattering

Janina Kneipp*†‡, Harald Kneipp*, and Katrin Kneipp*‡

*Wellman Center for Photomedicine, Harvard Medical School, Boston, MA 02114; and †Federal Institute for Materials Research and Testing, D-12489 Berlin, Germany

Communicated by Robert J. Silbey, Massachusetts Institute of Technology, Cambridge, MA, September 20, 2006 (received for review May 16, 2006)

Two-photon excitation is gaining rapidly in interest and significance in spectroscopy and microscopy. Here we introduce a new approach that suggests versatile optical labels suitable for both one- and two-photon excitation and also two-photon-excited ultrasensitive, nondestructive chemical probing. The underlying spectroscopic effect is the incoherent inelastic scattering of two photons on the vibrational quantum states called hyper-Raman scattering (HRS). The rather weak effect can be strengthened greatly if HRS takes place in the local optical fields of gold and silver nanostructures. This so-called surface-enhanced HRS (SEHRS) is the two-photon analogue to surface-enhanced Raman scattering (SERS). SEHRS provides structurally sensitive vibrational information complementary to those obtained by SERS. SEHRS combines the advantages of two-photon spectroscopy with the structural information of vibrational spectroscopy and the high-sensitivity and nanometer-scale local confinement of plasmonics-based spectroscopy. We infer effective two-photon cross-sections for SEHRS on the order of 10^{-46} to 10^{-45} cm^4·s, similar to or higher than the best ''action'' cross-sections (product of the two-photon absorption cross-section and fluorescence quantum yield) for two-photon fluorescence, and we demonstrate HRS on biological structures such as single cells after incubation with gold nanoparticles.

local optical fields | plasmonics | Raman spectroscopy | two-photon spectroscopy | biological structures

The probing of electronic or vibrational states in molecules by two photons provides several advantages over one-photon excitation, including the application of light of a longer wavelength and the limitation of the excitation volume in a sample (1, 2). These specific characteristics of two-photon excitation are of particular interest for biological applications of spectroscopy and microscopy. The development of optical probes that are suitable for two-photon excitation is therefore an important task in advancing optical techniques for biological applications. In addition, in biospectroscopy, another challenge is to obtain molecular structural information on biological samples and the development of methods to achieve this at high sensitivity, high lateral resolution *in situ* or *in vivo*, and without the need for purification.

In general, by the inelastic Raman scattering process, molecular vibrations and thereby molecular structure, composition, and interactions, can be detected by the observation of scattered light with a shifted wavelength compared with the wavelength of an excitation source. The Raman shift corresponds to the energy of the molecular vibration with which an excitation photon interacts. The fingerprint-like Raman spectral information has been used to study biological samples for decades and has gained popularity in particular in combination with microscopy, where it is used for multiparameter imaging of cells and tissues based on their intrinsic molecular composition (3–5). Hyper-Raman scattering (HRS), illustrated in a molecular level scheme in Fig. 1*a*, is a two-photon-excited Raman scattering process and thus results in Raman signals shifted relative to the doubled energy of the excitation laser (for an overview on HRS see refs. 6 and 7). The spectral information obtained in HRS is complementary to the information content of other vibrational (normal Raman and IR) spectra and therefore could be of use for a number of analytical applications. This is the case because HRS follows symmetry selection rules different from regular one-photon Raman scattering: HRS also probes IR-active vibrations that are usually not evident in Raman spectra and in addition can reveal so-called ''silent modes,'' vibrations that are seen neither in Raman nor in IR absorption spectra. Unfortunately, as a nonlinear, incoherent Raman process, HRS is an extremely weak effect with scattering cross-sections on the order of 10^{-65} cm^4·s, 35 orders of magnitude smaller than cross-sections of ''normal'' (one-photon-excited) Raman scattering and 15 orders of magnitude below typical two-photon absorption cross-sections. These extremely small cross-sections so far have precluded application of HRS as practical spectroscopic tool. To be observed, the effect requires very high excitation intensities provided in high-energy laser pulses (7) or, as recently demonstrated, by tightly focused femtosecond mode-locked lasers (8).

However, spectroscopic effects can be affected strongly when they take place in the immediate vicinity of metal surfaces and nanostructures because of coupling to surface plasmons (9). Based on resonances with their surface plasmons, gold and silver nanostructures also give rise to enhanced local optical fields. These local optical fields result in enhanced spectroscopic signals (10). Surface-enhanced Raman scattering (SERS) is one of the most impressive observations to demonstrate this effect (11, 12). Local optical fields also provide the key effect for the observation of so-called surface-enhanced HRS (SEHRS) signals from the molecules located in the nanometer-proximity of the nanostructures. The two-photon phenomenon of SEHRS is analogous to the enhancement of one-photon-excited Raman signals in SERS. Interestingly, HRS benefits even to a greater extent from the high local optical fields than normal Raman scattering does in the case of SERS, because of its nonlinear dependence on the (enhanced) excitation field. SEHRS has been demonstrated since the early days of SERS (13–15). Small aggregates, consisting of gold and silver nanoparticles and fractal structures of these metals that provide extremely strong field enhancement (16), can give rise to enhancement factors for HRS signals up to 20 orders of magnitude (17). The strong field enhancement can compensate for the extremely small cross-section of HRS and allows the measurement of SEHRS spectra at excitation intensities of 10^6 to 10^7 W·cm^{-2}, conditions that can be achieved easily with mode-locked picosecond lasers under weak focusing conditions (18) but also in tightly focused continuous wave (cw) (19) or low-energy pulsed lasers (20).

Author contributions: J.K., H.K., and K.K. designed research; J.K., H.K., and K.K. performed research; J.K. and H.K. analyzed data; and J.K. and K.K. wrote the paper.

The authors declare no conflict of interest.

Freely available online through the PNAS open access option.

Abbreviations: HRS, hyper-Raman scattering; SEHRS, surface-enhanced HRS; SERS, surface-enhanced Raman scattering; cw, continuous wave; GM, Goeppert-Mayer.

‡To whom correspondence may be addressed at: Harvard Medical School, 40 Blossom Street, Boston, MA 02114. E-mail: kneipp@usa.net or jkneipp@janina-kneipp.de.

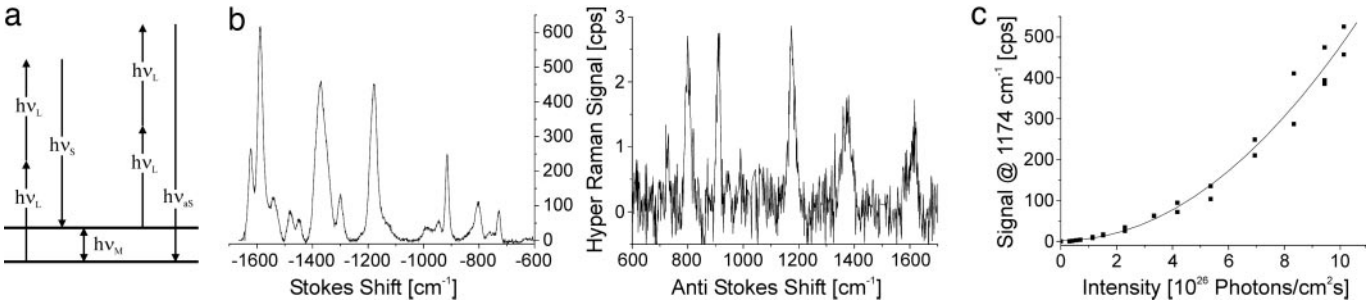

Fig. 1. SEHRS. (*a*) Schematic of the two-photon inelastic scattering process HRS: two near-IR photons $h\nu_L$ interact with a molecule. The results are scattering signals shifted relative to twice of the excitation energy by an amount equal to the vibrational energies of the molecule $h\nu_M$. Depending on whether the two photons interact with a molecule in its vibrational ground or first excited vibrational state, the scattering signals appear at the low-energy (Stokes, $h\nu_S$, left pair of arrows) or high-energy (anti-Stokes, $h\nu_{aS}$, right pair of arrows) side of the doubled excitation energy. (*b*) SEHRS Stokes and anti-Stokes spectra of 10^{-7} M of the dye molecule crystal violet attached to silver nanoaggregates in aqueous solution. The spectra were measured by using 1,064-nm mode-locked picosecond pulses at an average power of 40 mW (peak intensity 2×10^{25} photons $cm^{-2}{\cdot}s^{-1}$) and collection times of 10 and 60 s, respectively. Anti-Stokes scattering appears at much lower signal level than Stokes scattering, because the number of molecules in the excited vibrational state is much smaller than those in the vibrational ground state, but here anti-Stokes HRS can be observed because of the extremely high effective cross-section of SEHRS. In most practical bioanalytical applications and in the spectra shown in this article, the more intense, Stokes-shifted hyper-Raman light is used for label detection and molecular probing. (*c*) The square-law dependence of the HRS signal on the excitation intensity verifies the two-photon process. A logarithmic plot of the dependence of the SEHRS signal on excitation intensity shows a slope of 1.93 (plot not displayed here).

In this article, we report on two-photon-excited Raman scattering in the local optical fields of gold and silver nanostructures and demonstrate that its effective cross-sections can be higher than those of two-photon fluorescence. We show that these spectroscopic signals can be collected from single cells after incubation with gold nanoparticles, enabling two-photon probes with unique capabilities regarding sensitivity, molecular structural information content, specificity, photostability, and spatial localization.

Results and Discussion

The strong enhancement of the hyper-Raman signals in local optical fields enables that Stokes and also anti-Stokes SEHRS spectra of molecules such as the dye crystal violet (Fig. 1*b*) can be obtained at excitation intensities and concentrations that would rule out the measurement of HRS.

The scattering powers in SERS and SEHRS, P^{SERS} and P^{SEHRS}, measured in counts per second, can be estimated according to Eqs. **1a** and **1b** (see *Materials and Methods*). As a two-photon process, SEHRS depends quadratically on the excitation intensity (see Fig. 1*c*). From a comparison of the obtained scattering signals in SEHRS with SERS signals in the same sample, it can be inferred that effective cross-sections in SEHRS σ^{SEHRS} are 30 orders of magnitude smaller than effective SERS cross-section σ^{SERS}. The spectra in Fig. 2 *a* and *b* illustrate this finding for the example of the dye Rose Bengal. Assuming effective SERS cross-sections on the order of 10^{-16} cm^2, which were reported for several molecules (21–23), effective SEHRS cross-sections can be inferred to be on the order of 10^{-46} $cm^4{\cdot}s$, which corresponds to 10^4 Goeppert-Mayer (GM). These values are similar also for other molecules (compare the spectra of adenine in Fig. 4 discussed below). For comparison, most common fluorescence dyes have two-photon cross-sections in the range of 1–300 GM (1). Cross-sections for two-photon-excited luminescence of gold nanorods have been reported to be on the order of 10^3 GM (24). Webb and coworkers (25) recently have demonstrated cross-sections on the order of 10^4 GM for two-photon fluorescence of quantum dots.

The high enhancement level observed for SEHRS resulting in the high effective two-photon cross-sections can be explained by an extremely high field enhancement provided in the so-called "hot spots" of silver and gold nanostructures. In particular, high enhancement has been observed for nanoaggregates or nanoclusters formed by silver and gold colloidal particles (21, 23, 26). Fig. 3 shows SEHRS spectra of 10^{-8} M crystal violet on silver and gold nanoclusters. Despite different SERS enhancement factors for isolated nanoparticles of silver (10^6 to 10^7) and gold

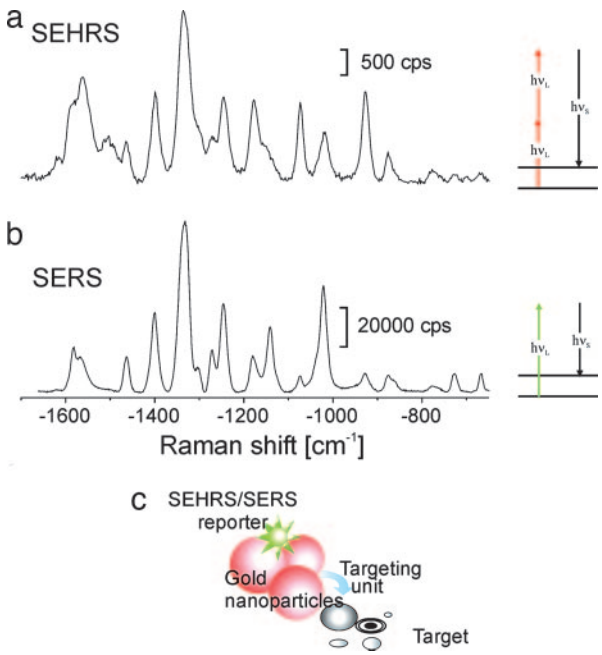

Fig. 2. Concept of labels based on SEHRS and SERS signals of reporter molecules linked to silver and gold nanoaggregates. (*a* and *b*) The example shows SEHRS (*a*) and SERS (*b*) spectra of 10^{-8} M Rose Bengal on silver nanoaggregates. Two-photon-excited SEHRS spectra were measured by using 1,064-nm mode-locked picosecond pulses (peak intensity, 8×10^{26} photons $cm^{-2}{\cdot}s^{-1}$). One-photon-excited SERS spectra were collected by using 785-nm cw light (intensity, 7×10^{21} photons $cm^{-2}{\cdot}s^{-1}$) SEHRS and SERS spectra were collected over 1 s and 0.1 s, respectively. For molecules showing low symmetry as the dye Rose Bengal, the spectral signatures of SERS and SEHRS are similar and differ in the relative intensities of some lines. For other molecules, however, there are drastic differences between the one-photon (SERS) and two-photon (SEHRS) spectrum (see Fig. 4). (*c*) Schematic of a SEHRS/SERS label. A reporter molecule is attached to a gold or silver nanostructure, which can be functionalized and directed to a specific target, e.g., a cellular compartment. The label is detected by the characteristic SEHRS/SERS fingerprint of the reporter molecule. $h\nu_S$, energy of the Raman Stokes-scattered photon; $h\nu_L$, excitation photon.

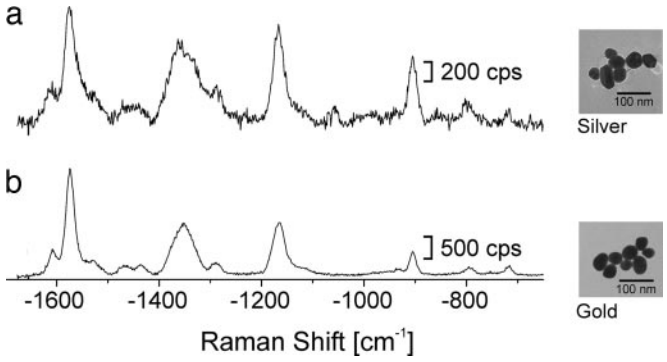

Fig. 3. SEHRS spectra of 10^{-8} M crystal violet on silver and gold nanoclusters by using 1,064-nm mode-locked picosecond pulses (peak intensity 10^{26} photons $cm^{-2}{\cdot}s^{-1}$). Examples for typical nanoaggregate structures are shown in the corresponding electron micrographs at *Right*. The strong SEHRS effect for gold suggests the use of gold nanoaggregates as biocompatible enhancing nanoparticles for two-photon-excited vibrational probing in biological structures (28).

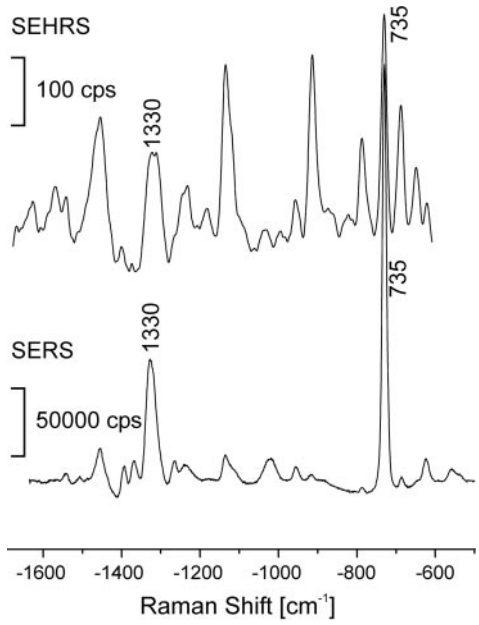

Fig. 4. SEHRS and SERS spectra of 10^{-6} M adenine in aqueous solution with silver nanoaggregates. One-photon-excited SERS spectra were measured by using 514.5-nm cw light (intensity, 7×10^{22} photons $cm^{-2}{\cdot}s^{-1}$). Two-photon-excited SEHRS spectra were measured by using 1,064-nm mode-locked picosecond pulses (7 ps, 78-MHz repetition rate; triangle pulse shape; intensity, 9×10^{26} photons $cm^{-2}{\cdot}s^{-1}$). SEHRS and SERS spectra were collected over 10 s and 0.1 s, respectively.

(10^3 to 10^4), measured at their plasmon resonances at 407 nm and 514 nm, respectively, the enhancement factors for nanoclusters or fractal structures are on the same order of magnitude for both metals at near-IR excitation. This result suggests the use of gold nanoaggregates as biocompatible, enhancing nanoparticles for two-photon-excited vibrational probing in biological structures, and it is particularly useful for the construction of new versatile optical two-photon labels for biological applications. Due to the basis of SEHRS, such a label is a hybrid, consisting of a reporter molecule that is linked to a nanostructure of silver or gold (schematic shown in Fig. 2*c*). Fig. 2*a* shows the spectrum of a SEHRS label using the biocompatible dye Rose Bengal as reporter. A label based on two-photon-excited Raman spectra (SEHRS) has a number of further advantages in addition to the extremely high effective two-photon scattering cross-sections: Compared with the broad and quite nonspecific spectral signatures known from fluorescence, a SEHRS spectrum comprises several narrow lines, specific for the molecular structure of the reporter. This high-molecular structural specificity of the vibrational spectrum can be used for a reliable detection of the two-photon label. Similar to the procedures demonstrated for SERS (27, 28), SEHRS has the capability of multiplex labeling and for utilization of spectral correlation methods that can improve the contrast for the detection of the label by microspectroscopy. As is evidenced by the SERS spectrum of the Rose Bengal label (Fig. 2*b*), labels based on SEHRS are not restricted to two-photon excitation in the near-IR but also are suitable for one-photon SERS detection in the near-IR and visible range.

Extremely strong SEHRS signals also are obtained for adenine (shown in Fig. 4), at two-photon excitation with 1,064-nm laser light. This molecule absorbs in the UV spectral region, and hence SEHRS cannot benefit from any one- or two-photon molecular electronic resonance contribution. The nonresonant nature of the two-photon scattering process implies that photodecomposition can be strongly reduced. Further, the excitation wavelength in a SEHRS experiment can be chosen independently of a specific reporter molecule or biochemical target, and rather be adapted to the requirements of the experimental system, in particular a specific biological sample.

Compared with the SERS spectrum of adenine (Fig. 4), its SEHRS spectrum shows several additional strong scattering lines that can be ascribed to IR-active vibrations (29). The signals obtained in SEHRS and SERS allow us to infer that the effective two-photon SEHRS cross-sections for the 1,330- and 735-cm^{-1} Raman lines are 1×10^{29} times and 6×10^{30} times smaller than their one-photon SERS cross-sections, respectively, (see *Materials and Methods* for estimate of ratios between effective SERS and SEHRS cross-sections). Taking into account that effective SERS cross-sections for adenine were shown to be on the order of 10^{-16} cm^2 (30), effective SEHRS cross-sections for adenine are between 10^{-46} and 10^{-45} $cm^4{\cdot}s$ (equal to 10^4 to 10^5 GM).

The example of adenine illustrates that effective SEHRS cross-sections (10^4 to 10^5 GM) can exceed by far the two-photon fluorescence cross-sections encountered for common biomolecules (31). These enormous SEHRS cross-sections for a native biomolecule provide the capability of label-free, sensitive two-photon chemical probing in a biological sample, such as a cell. After incorporation of gold nanoparticles, SEHRS spectra were acquired from individual macrophage cells of a cell culture (Fig. 5). Because the SEHRS spectrum is generated in the local optical fields of the gold nanoparticles, the dimensions of the probed volumes in the cells are determined by the confinement of the local optical fields, which is two orders of magnitude smaller than the dimensions determined by the diffraction limit (26). The example spectra (Fig. 5*a*) give evidence of proteins, lipid molecules, and also nucleic acid components that are part of the nanoenvironment of different nanoparticles in the endosomal system of the cell. As discussed above, a two-photon-excited Raman spectrum follows different selection rules. Therefore, SEHRS spectra of a cell contain features that are absent from other Raman spectra, e.g., a pronounced amide II signal of proteins usually detected by IR absorption spectroscopy (Fig. 5*b*), a method which is hampered by very low (≈ 10 μm, because it is diffraction-limited) lateral resolution. Interestingly, SEHRS also observes spectral bands above 1,800 cm^{-1}, which are likely combination modes. The spectral region between 1,800 and 2,700 cm^{-1} is almost featureless in other vibrational (Raman and IR) spectra of cells and tissues.

To summarize, our studies demonstrate the extension of SERS-based concepts in biospectroscopy to two-photon excita-

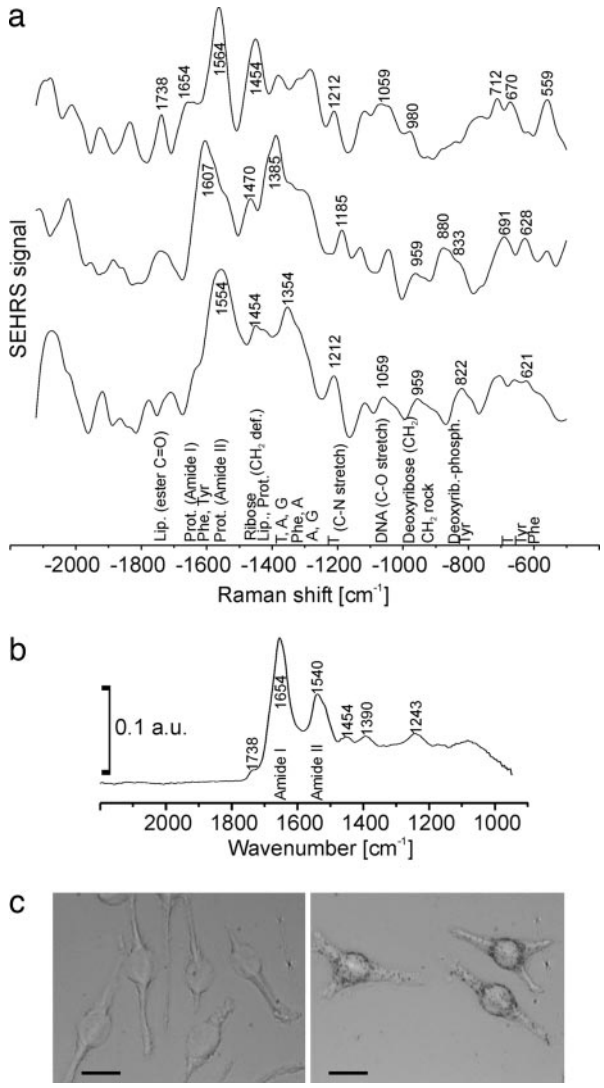

Fig. 5. Application of SEHRS to collect intrinsic biochemical information from nanometer-scaled volumes in individual cultured cells. (*a*) SEHRS spectra measured from dry J 774 cells after 4-h uptake of gold nanoparticles. Excitation was achieved by using 1,064-nm mode-locked picosecond pulses, average power 30 mW, size of the laser spot ≈1 μm, and collection time 10 s. The spectra were measured at different, randomly chosen locations in the cell where gold nanoaggregates (compare with Fig. 3) must have been present in order for SEHRS to occur. Vibrational bands were assigned after refs. 3, 35, and 36 to major contributing molecules and molecular groups present in the nanometer-proximity of the gold nanoaggregates, indicated below the spectra. (*b*) For comparison, shown is an example of an IR spectrum of a dried J 774 cell on CaF_2 substrate. The IR spectrum was acquired from a ≈30-μm-diameter spot. (*c*) Micrographs of fixed J 774 cells after 4-h incubation with the gold nanoparticles (*Right*) and corresponding controls (*Left*). (Scale bars, 20 μm.) a.u., absorbance units; Lip., lipids; Prot., proteins; stretch, stretching vibration; def., deformation; rock, rocking vibration.

tion, namely SEHRS. The approach suggests highly efficient two-photon labels based on the SEHRS signature of a reporter molecule on gold or silver nanoaggregates as well as two-photon vibrational spectroscopy of biological matter. For nondestructive chemical probing in cells, SEHRS combines the advantages of two-photon spectroscopy with the structural information of vibrational spectroscopy and the high sensitivity and nanometer-scale local confinement of plasmonics-based spectroscopy. For the spectroscopic characterization and microspectroscopic imaging of cells and tissues, the greatly reduced possible photoxicity and stress to the sample because of longer wavelengths excitation, as well as the confinement of the two-photon interaction to the focus of the laser beam, are major advantages. Depending on the substructure of interest in a cell or other biological system, functionalization of gold nanoparticles for targeted probing can be undertaken based on established methods used for electron microscopy and other labeling methods (32, 33). Effective two-photon cross-sections higher than those obtained for two-photon fluorescence, as well as the unique capability of probing vibrational modes that are usually not seen in high lateral resolution microscopy or that are absent from other vibrational spectroscopic data, make SEHRS a promising spectroscopic tool for bioanalytical applications and molecular structural probing.

Materials and Methods

Preparation of Enhancing Nanostructures. Silver and gold nanoparticles in a size range between 20 and 50 nm were produced by chemical preparation as described in ref. 34, resulting in isolated nanoparticles but also small aggregates in a colloidal solution. Enhancing nanostructures in the SEHRS experiments are nanoaggregates at 100- to 200-nm minimum size. These small clusters can generate extremely high local optical fields, and, in the presence of 10^{-2} M NaCl, such clusters provide SERS enhancement factors enabling single-molecule Raman detection at nonresonant near-IR excitation (21, 26).

Sample Preparation. Crystal violet, Rose Bengal, and adenine (all purchased from Sigma, St. Louis, MO) were prepared in 10^{-5} M stock solutions and added to the aqueous solution of silver and gold nanoclusters for final concentrations between 10^{-7} and 10^{-8} M.

SEHRS Experiments. In the reported experiments, SEHRS spectra were measured by using mode-locked near-IR lasers operating at average powers between 10 mW and 3 W (1,064 nm, 7-ps pulses FWHM, triangle pulse shape, 78-MHz repetition rate). In SEHRS studies performed in solutions, weak focusing conditions were applied by using spot sizes of ≈100 μm. These experimental parameters result in excitation intensities between 10^5 and 10^8 W·cm^{-2}, corresponding to photon flux densities on the order of 10^{24} to 10^{27} photons cm^{-2}·s^{-1}. The scattered light was collected in 90° or in backward direction. A single-stage spectrograph and a liquid nitrogen-cooled CCD detector were used for spectral dispersion and detection of the scattered light. Holographic notch filters for 1,064 nm and 532 nm in front of the entrance slit were used to reject Rayleigh and hyper-Rayleigh light. SEHRS spectra were collected over durations between 100 ms and 10 s, depending on the applied excitation intensities and concentrations of the analyte molecules. Laser pulse lengths of 7 ps ensured the observation of well resolved hyper-Raman spectra composed from narrow hyper-Raman lines without any broadening effect attributable to the spectral width of the excitation laser.

For comparison between two-photon-excited SEHRS and one-photon-excited SERS, SERS spectra were measured at 785-nm cw excitation from a diode laser or with 541-nm cw argon ion laser excitation.

For SEHRS studies in cells, the experimental conditions were modified so that all measurements could be conducted with a microspectroscopic setup (28). The 1,064-nm excitation laser was focused to a spot of ≈1 μm on the sample, resulting in peak intensities of ≈5×10^{28} photons cm^{-2}·s^{-1}. A microscope objective was used to direct the laser light onto microscope coverslips holding the dry-fixed cultured cells. The same objective also was used to collect the scattered hyper-Raman light and for further projection onto the spectrometer described above. The microscope was equipped with a computer-controlled x, y mapping stage, and spectra were collected from several randomly chosen

spots with collection times of 10 s. Spectra from the control cells were obtained in a raster-scan fashion at a step size of 2 μm. Because of the absence of gold nanoparticles in the control cells, no Raman or hyper-Raman signals were detected in controls.

Estimate of Effective Two-Photon Scattering Cross-Sections. The scattering power in SERS and SEHRS P^{SERS} and P^{SEHRS} measured in counts per second was estimated according to

$$P^{\mathrm{SERS}} = N_0 \sigma^{\mathrm{SERS}} n_L \qquad [1a]$$

and

$$P^{\mathrm{SERS}} = N_0 \sigma^{\mathrm{SEHRS}} n_L^2, \qquad [1b]$$

where $\sigma SERS$ and $\sigma SEHRS$ are the effective cross-sections in SERS and SEHRS, respectively. N_0 is the number of molecules contributing to the signal, and n_L is the excitation intensity (photons $\mathrm{cm}^{-2}\cdot\mathrm{s}^{-1}$) for SERS and SEHRS, respectively (17, 29). Knowing the excitation intensities, a comparison between SEHRS and SERS signals measured from the same sample allows to estimate a ratio of effective cross-sections in two-photon SEHRS and one-photon SERS based on Eqs. **1a** and **1b** for SERS and SEHRS, respectively. Note that for this estimate it has to be considered that the scattering power (photons per second) measured in SEHRS is an average over the collection time and has to be corrected according to the duty cycle of the excitation laser (product of repetition rate and pulse length). The effective two-photon cross-section for SEHRS is inferred from this ratio and from the SERS cross-sections reported in the literature (21–23).

Preparation of Cultured Cells for SEHRS Experiments. Cells of the cell line J774 (kind gift of T. Hasan, Wellman Center for Photomedicine) were grown in DMEM culture medium containing 10% FCS in a humidified incubator (37°C, 5% CO_2). Before reaching confluence, they were split and grown in six-well plates on flamed coverslips. When the cells reached ≈80% confluence, the culture medium was replaced with medium diluted with gold nanoparticle suspension (1:2) containing 5×10^{-11} M gold nanoparticles. Control slides were incubated with medium diluted in PBS. To allow uptake of the nanoparticles by the cells, the plates were incubated in their regular growth environment for 4 h. After this incubation period, the medium was removed, and the cells were washed thoroughly with PBS containing Ca^{2+} und Mg^{2+} (Mediatech, Herndon, VA). Some of the coverslips were fixed in 4% paraformaldehyde, followed by a 5-min incubation in cold methanol. The fixed cells were inspected with a ×60 microscope objective (Olympus, Center Valley, PA). Uptake of high numbers of gold nanoparticles was verified by the appearance of black spots in the bright-field images (Fig. 5*c*), indicating accumulations of the nanoparticles, and by the ability to measure SEHRS and SERS spectra from the cells. For the SEHRS experiments, the other coverslips were washed in PBS and immersed very briefly (≈1 s) in water before they were placed upright in a desiccator, which then was evacuated quickly to remove all water from the slides within seconds. This fast drying process assures stable fixation of the cells without the need to apply further chemicals that could modify or dissolve the cells' molecular composition.

Measurement of IR Spectra from J774 Cells for Comparison. We acquired Fourier-transform IR (FTIR) absorption spectra (e.g., example in Fig. 5*b*) from J774 cells for comparison of SEHRS spectral information with that of other vibrational spectroscopies. The cells were incubated and fixed as described above but grown on CaF_2 slides rather than on standard glass coverslips. FTIR spectra were measured with an IR-Scope II, coupled to an IFS66/v FTIR spectrometer (both from Bruker Optics, Billerica, MA) and by using the ANKA synchrotron (Karslruhe, Germany) as the IR source. Spectra were measured from spot sizes of 30 μm, averaging 512 interferograms to yield one spectrum.

We thank R. Peteranderl for help with cell growing and T. Hasan for providing space in her cell culture facility. J.K. acknowledges ANKA Angstroemquelle Karlsruhe for the provision of beam time and thanks D. Moss and M. Süpfle for assistance with beamline ANKA-IR. This work was supported by Department of Defense Grant AFOSR FA9550-04-1-0079 and by the generous gift of Dr. and Mrs. J. S. Chen to the optical diagnostics program of the Massachusetts General Hospital Wellman Center for Photomedicine.

1. Zipfel WR, Williams RM, Webb WW (2003) *Nat Biotechnol* 21:1368–1376.
2. So PTC, Dong CY, Masters BR, Berland KM (2000) *Annu Rev Biomed Eng* 2:399–429.
3. Peticolas WL, Patapoff TW, Thomas GA, Postlewait J, Powell JW (1996) *J Raman Spectrosc* 27:571–578.
4. van Manen, H-J, Kraan YM, Roos D, Otto C (2005) *Proc Natl Acad Sci USA* 102:10159–10164.
5. Hanlon EB, Manoharan R, Koo TW, Shafer KE, Motz JT, Fitzmaurice M, Kramer JR, Itzkan I, Dasari RR, Feld MS (2000) *Phys Med Biol* 45:R1–R59.
6. Denisov VN, Mavrin BN, Podobedov VB (1987) *Phys Rep* 151:1–92.
7. Ziegler LD (1990) *J Raman Spectrosc* 21:769–779.
8. Shimada R, Kano H, Hamaguchi HO (2006) *Optics Lett* 31:320–322.
9. Chance RR, Prock A, Silbey R (1974) *J Chem Phys* 60:2744–2748.
10. Moskovits M (1978) *J Chem Phys* 69:1459–1461.
11. Jeanmaire DL, Duyne RPV (1977) *J Electroanal Chem* 84:1–20.
12. Albrecht MG, Creighton JA (1977) *J Am Chem Soc* 99:5215–5217.
13. Murphy DV, Von Raben KU, Chang RK, Dorain PB (1982) *Chem Phys Lett* 85:43–47.
14. Golab JT, Sprague JR, Carron KT, Schatz GC, van Duyne RP (1988) *J Chem Phys* 88:7942–7951.
15. Nai-Teng Y, Shuming N, Lipscomb LA (1990) *J Raman Spectrosc* 21:797–802.
16. Stockman MI, Shalaev VM, Moskovits M, Botet R, George TF (1992) *Phys Rev B* 46:2821–2830.
17. Kneipp K, Kneipp H, Itzkan I, Dasari RR, Feld MS (1999) *Chem Phys* 247:155–162.
18. Kneipp H, Kneipp K, Seifert F (1993) *Chem Phys Lett* 212:374–378.
19. Itoh T, Ozaki Y, Yoshikawa H, Ihama T, Masuhara H (2006) *Appl Phys Lett* 88:084102.
20. Weinan L, Meyers-Kelley A (2006) *J Am Chem Soc* 128:3492–3493.
21. Kneipp K, Wang Y, Kneipp H, Itzkan I, Dasari RR, Feld MS (1996) *Phys Rev Lett* 76:2444–2427.
22. Nie S, Emory SR (1997) *Science* 275:1102–1106.
23. Michaels AM, Nirmal M, Brus LE (1999) *J Am Chem Soc* 121:9932–9939.
24. Wang HF, Huff TB, Zweifel DA, He W, Low PS, Wei A, Cheng JX (2005) *Proc Natl Acad Sci USA* 102:15752–15756.
25. Larson DR, Zipfel WR, Williams RM, Clark SW, Bruchez MP, Wise FW, Webb WW (2003) *Science* 300:1434–1436.
26. Kneipp K, Kneipp H, Kneipp J (2006) *Acc Chem Res* 39:443–450.
27. Cao YWC, Jin RC, Mirkin CA (2002) *Science* 297:1536–1540.
28. Kneipp J, Kneipp H, Rice WL, Kneipp K (2005) *Anal Chem* 77:2381–2385.
29. Kneipp H, Kneipp K (2005) *J Raman Spectrosc* 36:551–554.
30. Kneipp K, Kneipp H, Kartha VB, Manoharan R, Deinum G, Itzkan I, Dasari RR, Feld MS (1998) *Phys Rev E* 57:R6281–R6284.
31. Xu C, Zipfel WR, Shear JB, Williams RM, Webb WW (1996) *Proc Natl Acad Sci USA* 93:10763–10768.
32. Tkachenko AG, Xie H, Liu YL, Coleman D, Ryan J, Glomm WR, Shipton MK, Franzen S, Feldheim DL (2004) *Bioconjug Chem* 15:482–490.
33. Wu X, Liu H, Liu J, Haley KN, Treadway JA, Larson JP, Ge N, Peale F, Bruchez MP (2003) *Nat Biotechnol* 21:41–46.
34. Lee PC, Meisel D (1982) *J Phys Chem* 86:3391–3395.
35. Parker FS (1983) *Applications of Infrared, Raman, and Resonance Raman Spectroscopy in Biochemistry* (Plenum, New York).
36. Puppels GJ, Mul, F. F. M. D., Otto C, Greve J, RobertNicoud M, Arndt-Jovin DJ, Jovin T (1990) *Nature* 347:301–303.